Journal of Controlled Release 360 (2023) 772–783

Contents lists available at ScienceDirect

Journal of Controlled Release

journal homepage: www.elsevier.com/locate/jconrel

Rational nanoparticle design: Optimization using insights from experiments and mathematical models

Owen Richfield [a], Alexandra S. Piotrowski-Daspit [a,1], Kwangsoo Shin [a,2], W. Mark Saltzman [a,b,c,d,*]

[a] Department of Biomedical Engineering, Yale University, New Haven, CT 06511, USA
[b] Department of Cellular & Molecular Physiology, Yale University, New Haven, CT 06511, USA
[c] Department of Chemical & Environmental Engineering, Yale University, New Haven, CT 06511, USA
[d] Department of Dermatology, Yale University, New Haven, CT 06511, USA

ARTICLE INFO

Keywords:
Rational nanoparticle design
Polymeric nanoparticles
Nanoparticle pharmacokinetics
Physiologically based pharmacokinetics
Multiscale mathematical modeling

ABSTRACT

Polymeric nanoparticles are highly tunable drug delivery systems that show promise in targeting therapeutics to specific sites within the body. Rational nanoparticle design can make use of mathematical models to organize and extend experimental data, allowing for optimization of nanoparticles for particular drug delivery applications. While rational nanoparticle design is attractive from the standpoint of improving therapy and reducing unnecessary experiments, it has yet to be fully realized. The difficulty lies in the complexity of nanoparticle structure and behavior, which is added to the complexity of the physiological mechanisms involved in nanoparticle distribution throughout the body. In this review, we discuss the most important aspects of rational design of polymeric nanoparticles. Ultimately, we conclude that many experimental datasets are required to fully model polymeric nanoparticle behavior at multiple scales. Further, we suggest ways to consider the limitations and uncertainty of experimental data in creating nanoparticle design optimization schema, which we call quantitative nanoparticle design frameworks.

1. Introduction

Nanoparticles (NPs) of myriad size and composition have been explored for a wide array of potential functions in medicine [1,2]. Some of these NP formulations are now available for clinical use [3]. Drug-encapsulating NPs (also called 'nanocarriers') have been developed to reduce drug side-effects, enhance drug accumulation at the target site (s), and deliver biologically fragile cargo such as nucleic acids [4,5]. Polymeric NPs are a class of NP composed of (typically biodegradable) polymers (*e.g.* poly(lactic-*co*-glycolic acid), or PLGA). Drug release kinetics are based on the material and functional properties of the component polymers [6]. By altering the polymer composition, such as by incorporating poly(ethylene glycol) (PEG) into the polymer backbone to create amphipathic PLGA-PEG block copolymers, it is possible to drastically alter the pharmacokinetics of the resulting NPs [4,7].

The families of biodegradable polymers and their variants afford a great deal of versatility in polymeric NP design; NP shape, size, surface charge, and degradation rate are readily tunable [8–12]. Furthermore, polymeric NPs are eligible for numerous surface modifications including the conjugation of targeting moieties such as antibodies [13–15]. It is known that 'NP characteristics'—which generally refers to the physicochemical properties of polymers and resulting NPs—have varying influence on NP pharmacokinetics [16–22], particularly when those properties influence the NP surface. Thus, finding an optimal polymeric NP formulation with the desired pharmacokinetic profile for a particular application is of intense research and clinical interest [6]. As a salient example, Hrkach et al. [23] used a library of over 100 polymeric NP formulations to optimize the pharmacokinetic profile of a docetaxel-loaded, prostate cancer-targeted NP. In this case, the NP size, polymer content (PLGA, polylactic acid (PLA), and PLGA-PEG), polymer

* Corresponding author at: Department of Biomedical Engineering, Yale University, New Haven, CT 06511, USA.
E-mail address: mark.saltzman@yale.edu (W.M. Saltzman).
[1] Present address: Department of Biomedical Engineering and Department of Internal Medicine – Pulmonary and Critical Care Medicine Division, University of Michigan; Ann Arbor, Michigan, USA.
[2] Present address: Department of Polymer Science and Engineering and Program in Environmental and Polymer Engineering, Inha University; Incheon, Republic of Korea.

https://doi.org/10.1016/j.jconrel.2023.07.018
Received 15 March 2023; Received in revised form 22 June 2023; Accepted 8 July 2023
Available online 22 July 2023

molecular weight, surface ligand density, surface hydropholicity, and drug loading/release kinetics were combinatorially evaluated in terms of their impact on the NP pharmacokinetics in rats and tumor-bearing mice.

Generally speaking, the search for an 'optimal' polymeric NP formulation has been conducted through two lines of investigation: experimentation and mathematical modeling. Experiments are crucial for the elucidation of the physiological mechanisms that impact polymeric NP pharmacokinetics, such as NP-immune cell interactions. But the throughput of these experiments is necessarily limited by time and materials; an exhaustive, combinatorial experimental study of NP characteristics and their pharmacokinetic influence is bound to be limited in scope. In the above example from Hrkach [23], the physicochemical characteristics of the docetaxel-loaded NPs were optimized based on *in vitro* drug release kinetics, not *in vivo* pharmacokinetics. Thus, due to the necessarily low throughput of *in vivo* studies, other strategies (such as extrapolating *in vitro* results to *in vivo* behaviors) are necessary to try to predict NP pharmacokinetics. On the other hand, mathematical modeling is relatively inexpensive in time and materials, and can theoretically evaluate the pharmacokinetic influence of each NP characteristic in a combinatorial manner. But given the spatiotemporal complexity of NP circulation in a complex organism, models are challenged to reproduce often highly nonlinear phenomena that are not known or well understood. To this end, multiscale mathematical models of NP delivery consider the physical aspects of NP transport at all relevant biological scales (*i.e.* organism, organs, blood vessels, and cells) [24].

The promise of mathematical modeling in NP development is 'rational NP design,' wherein mathematical and/or computational models are used to predict the NP characteristics that will optimize pharmacokinetics for a particular drug delivery application [25]. This form of optimization is valuable for improving the efficacy of the delivered therapy, and for optimizing NP formulations for regulatory and/or manufacturing purposes, both of which are crucial aspects of clinical translation [26]. A substantial obstacle to the realization of rational NP design is the need for experimental validation and uncertainty quantification of model results; in other words, once a model is created, how do we know it is correct? And if it is correct, how much can we trust that model's predictions? Model accuracy is a function of the data used to parameterize the model as well as the certainty of that data, which is dependent upon the experimental methods.

In this cross-sectional review, we discuss polymeric NP pharmacokinetics from both experimental and mathematical modeling perspectives. We evaluate the advantages and disadvantages of the methodologies used in each context by discussing the inherent uncertainty of experiments and relative quantitation of NP biodistribution, and the challenges associated with modeling NP delivery at multiple scales. Finally, we make the case that, especially for polymeric NPs, a combined experimental-computational approach has the potential to realize rational NP design through the creation of quantitative NP design frameworks.

2. Polymeric NP biodistribution and pharmacokinetics

Drug-loaded polymeric NPs, by virtue of their size and composition, show distinct differences from small molecule drugs in terms of their pharmacokinetics; water-soluble drugs are typically filtered at the renal glomerulus or secreted by the tubules and thus are continually removed from circulation [27]. Due to their size (~100nm diameter), polymeric NPs are rarely excreted in the urine [18]. Instead, NPs are degraded in the liver and/or excreted through the biliary stream [28]. While most non water-soluble drugs are metabolized in hepatocytes [29], the vast majority of NPs administered in one dose will be taken up by macrophages and other phagocytic cells in organs such as the liver and spleen [18] and/or tumors [30,31]. Thus, systemic NP pharmacokinetics, biodistribution and targeting are highly dependent upon NP-phagocyte interactions.

There are two general experimental methodologies by which the pharmacokinetics and biodistribution of polymeric NPs are characterized (Fig. 1): fluorescence quantification, which relies on a fluorescent dye that is loaded into the NP, usually during formulation [32], and activity quantification, which relies on the incorporation of a radioactive isotope in the NP formulation [33]. The primary advantage of using fluorescence to quantify NP uptake in different tissues is the ease with which fluorescent dyes are handled, incorporated into the NP core, and quantified. Fluorescence can be quantified with several methods, including fluorescence imaging using an *in vivo* imaging system (IVIS) or optical epifluorescence microscope, liquid-liquid extraction quantification (LLEQ), and flow cytometry of organ or blood cells [34,35] [36].

In LLEQ, the fluorescent dye encapsulated within polymeric NPs is extracted from homogenized organs using an organic solvent (*e.g.* chloroform or dimethylsulfoxide) to dissolve the polymer components, and then quantified based on standard curves drawn from known titrations of fluorescent NPs read using a plate reader. Although this NP quantification strategy is subject to biases introduced in the organ homogenization process, LLEQ is considered more quantitative than IVIS imaging, as we describe in later sections [37]. It is currently unknown to what extent flow cytometry accurately quantifies NP uptake in different organs and/or cell types. Work from our laboratory has shown the utility of fluorescence microscopy in quantifying fluorescent NP concentration in blood [36], which provides a quantitative basis for studying NP pharmacokinetics based on the NPs' fluorescence intensity alone. We have also employed quantitative fluorescence microscopy to estimate the endothelial cell coverage by targeted NPs in perfused human organs [13,14].

There are several methods by which organ and/or blood NP concentration can be quantified without using NP fluorescence. Metallic (*i.e.* gold, nickel and cobalt) NP concentration can be readily quantified using inductively coupled plasma atomic emission spectroscopy (ICP-AES) or ICP mass spectroscopy (ICP-MS), after nitric acid digestion of cells and tissues [38], however this method does not apply to polymeric NPs. The most efficient methodology to trace polymeric NP biodistribution and pharmacokinetics *in vivo* (without relying on fluorescence intensity quantification) is to chelate a radioisotope to the NP surface [39,40] or incorporate the radioisotope into the polymer backbone [41]. Since the high energy gamma rays emitted by the radioisotope can penetrate biological tissue with minimal attenuation and their signals are independent from the NPs' environment, radioisotopes have been a great tool for quantification of NP accumulation *in vivo*. Positron emission tomography (PET), and single positron emission computed tomography (SPECT) have been used to image radioisotopes *in vivo* and *ex vivo* after animal sacrifice and organ retrieval. Gill et al. demonstrated the utility of radioisotope conjugation to the NP surface to develop a theranostic NP in which the ^{111}In isotope conjugated to the NP surface serves as both an imaging contrast agent and a radiotherapy for esophageal cancer [39]. The challenge with this methodology for tracking NP pharmacokinetics and biodistribution is the crucial factor of polymeric NP degradation, such that a surface-conjugated radioisotope may separate from the NP and distribute differently than the NP core [42]. The kinetics of polymer degradation are likely to differ between NP formulations and polymer types.

The role of NP physicochemical properties in NP pharmacokinetics has been the focus of numerous reviews [16–22]. NP size and composition are the first variables to consider as they are directly related to NP formulation, whereas surface properties either emerge from NP formulation or are engineered after-the-fact. In general, NP size modulates pharmacokinetics and biodistribution; independent of material and surface charge, larger NPs (diameter $>$ 100 nm) exhibit increased accumulation in the spleen and liver [43], while smaller NPs (diameter $<$ 10 nm) exhibit clearance by the kidneys [18]. NP size also impacts targeting; NPs with diameter ~ 50 nm exhibit distinct increases in uptake by the mesangium of glomeruli, whereas larger ~100 nm diameter

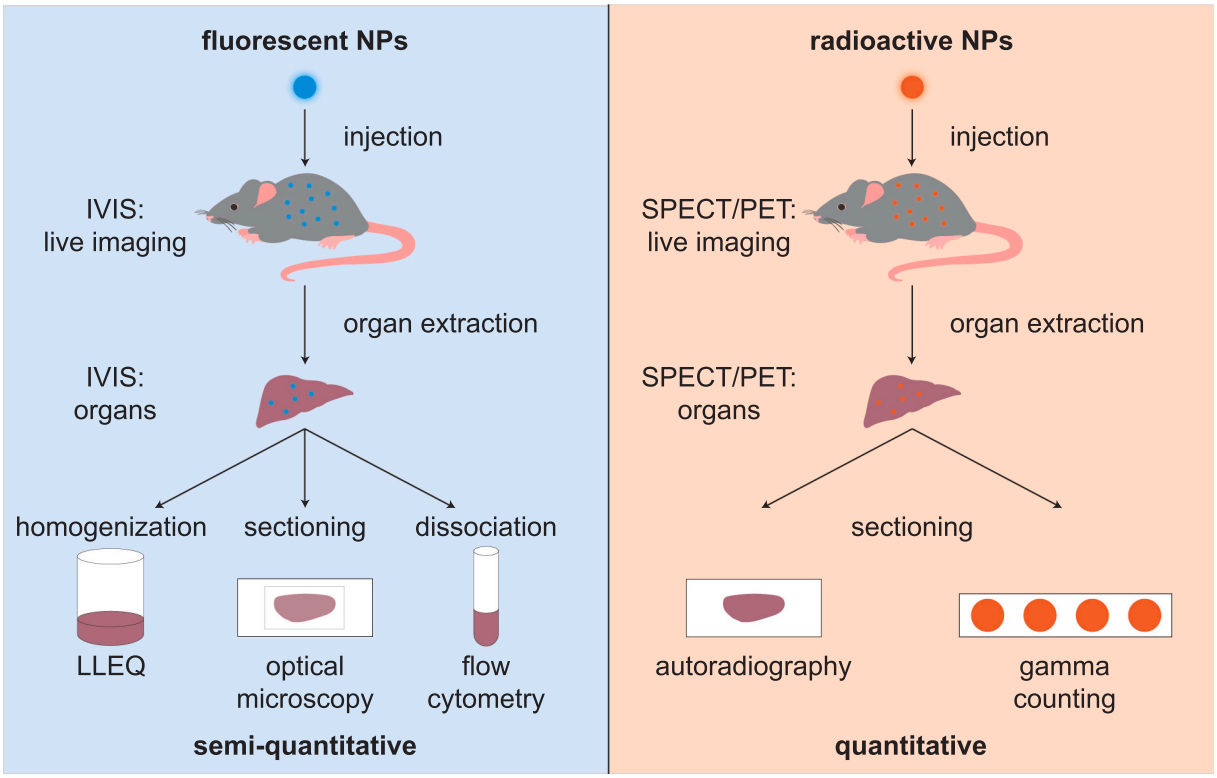

Fig. 1. Experimental methods of NP pharmacokinetics and biodistribution quantification. Semi-quantitative methods of fluorescence quantification (left) are used for measuring the biodistribution of fluorescent NPs while more quantitative methods of activity quantification (right) are used for measuring biodistribution of radioactive NPs.

NPs exhibit substantially less accumulation in renal corpuscles [44]. Work from our laboratory has shown that tuning PLGA NP size significantly impacts their biodistribution, wherein large NPs (diameter > 200 nm) are mostly sequestered in the liver and spleen while small NPs (diameter ~ 120 nm) show greater uptake in lung and bone marrow [45]. The material properties of NPs substantially impact their pharmacokinetics; Ogawa et al. [46] showed that tuning the PEG isomer and PLA molecular weight directly impacted the NP stability in circulation and drug release kinetics. In an *in vitro* complement activation assay, D'Addio et al. [47] showed that polycaprolactone (PCL) NPs significantly activated the complement system for PCL with a molecular weight of 9 kDa, but not 5 kDa.

Of all NP characteristics, surface properties are the most salient to their interaction with cells in the blood and tissues. Numerous strategies have been developed to alter NP surface properties [48]. Using a polydopamine coating, Liu et al. [9] developed NPs with surface modifications—including bovine serum albumin (BSA) conjugation, PEGylation, and poly-L-lysine (PLL) surface coating—each of which had distinct pharmacokinetic and/or therapeutic effects. Zhou et al. [49] showed that functionalizing NPs with particular PEG structures (hierarchical, linear, and others) could selectively tune NP uptake in non-Kupffer liver cells. Our laboratory demonstrated that NP surface topographical modification alters NP-cell interactions [50], pharmacokinetics, and immunogenicity [35]. In the latter study, coated PLA NPs with hyperbranched polyglycerol (PG) and linear PG were used to demonstrate that the blood circulation time (augmented by NPs escaping the immune system) strongly depends on not only the surface density of the grafted polymer but also the structure of the grafted polymers.

One of the most significant means by which NP surface modification impacts pharmacokinetics and biodistribution is by surface effects on protein corona formation [48]. The formation of a protein corona on the surface of NPs is a key step in the process of NP uptake by macrophages; corona formation can be altered by PEGylating the NP surface [51]. Bertrand et al. [41] showed that ApoE, a serum protein adsorbed to PLGA-PEG NPs in the mouse circulation, increases the circulation time of these NPs and can be modulated by PEG coverage. Cao et al. [52] estimated the protein-NP association constant K_A for a series of increasingly PEGylated PLA NPs, and showed that the K_A is negatively correlated with circulation time of the NPs and positively correlated with Kupffer cell uptake in the liver.

Targeting moieties are another powerful surface modification for altering NP pharmacokinetics. Folic acid-conjugated NPs have been utilized to improve NP delivery to tumors [31,53] and the kidney [54]. To target proximal tubule cells in mice, Ordikhani et al. [55] conjugated Lambda light chains to the surface of PEGylated PLGA NPs. Antibodies have been conjugated to the surface of PLA-PEG NPs in our laboratory to more efficiently target endothelial cells *in vitro* and in *ex vivo* normothermically perfused human kidneys [14,15]. In these studies, EDC-NHS chemistry was used to conjugate the Fc portion of CD31 antibodies to the PLA-PEG NP surface. A second study from our laboratory used a monobody protein as an adapter between the NP and the antibody Fc portion, improving the orientation of the antibody and enhancing endothelial cell targeting significantly [13].

3. Physiologically based pharmacokinetics of polymeric NPs

Physiologically based pharmacokinetics (PBPK) is a common mathematical modeling approach utilized in predicting drug or NP pharmacokinetics at the whole-body scale [56–58]. These methods have been used for decades to model and predict the pharmacokinetic behavior of chemotherapeutics and other drugs [59], but PBPK models of NPs are relatively new. In general, NP PBPK models represent physiological spaces (organs, tumors, blood, non-blood fluids) as compartments in which the NP concentration changes over time. Mathematically, the NP concentration in each compartment is modeled as an ordinary

differential equation that uses mass conservation to estimate NP uptake and output (Fig. 2A). NPs are distributed throughout the compartmental system with rate constants that describe NP transport between blood and organ compartments. For PBPK models where each organ is modeled with two sub-compartments (intravascular and extravascular), NP accumulation in the extravascular space is assumed to be limited by either NP delivery to the organ ('blood flow-limited') or by the NP interactions with the cells in the organ ('membrane-limited'). These cases correspond to different systems of equations to describe NP accumulation; a blood flow-limited model assumes NPs reach equilibrium between blood and tissue, instantaneously. Mathematically, this means that the concentration of drug in the extravascular and intravascular sub-compartments, denoted C_E and C_I, respectively, can be represented as:

$$V_I\frac{dC_I}{dt} = Q_I(C_P - C_I) - N \tag{1}$$

$$V_E\frac{dC_E}{dt} = N - fC_E$$

where Q_I denotes the intravascular blood flow in the organ, C_P denotes the plasma NP concentration, fC_E denotes the clearance of NPs from the extravascular tissue, V_I and V_E denote the intravascular and extravascular volumes, respectively, and intra-organ NP flux is represented by a constant flux parameter, N [59]. Membrane-limited models assume that the absorption of NPs into the extravascular space is slower than the rate of NP delivery in the blood. NP concentration is assumed to not immediately reach equilibrium between organ sub-compartments:

$$V_I\frac{dC_I}{dt} = Q_I(C_P - C_I) - PA\left(\frac{C_I}{K} - C_E\right) \tag{2}$$

$$V_E\frac{dC_E}{dt} = PA\left(\frac{C_I}{K} - C_E\right) - fC_E$$

where K is the equilibrium constant:

$$K = \left(\frac{C_I}{C_E}\right)_{eq} \tag{3}$$

And PA is the permeability-area product. Membrane-limited models fit NP pharmacokinetic data substantially better than blood flow-limited models [7], indicating the (intuitively) important role of the cell membrane as a barrier to NP uptake.

While membrane-limited models are helpful for predicting the bulk accumulation of NPs in different organ compartments, these models do not incorporate cell type-specific NP transport properties. In this case, we define cell NP transport as the binding and internalization of NPs at the cell membrane. Some cells are more likely to take up NPs than others; for example, in certain organs, macrophages and other phagocytic cells act as a 'sink' that sequester NPs. But phagocytic cells are not always the intended target for NP-encapsulated drugs. Phagocyte-incorporated models use sub-compartments to describe NP transport between intravascular, tissue and phagocytic spaces within each organ (Fig. 2B). This model structure allows for the estimation of the degree to which NPs are taken up by phagocytes and, therefore, do not reach the other cells in the tissue. This model structure also increases the number of parameters required to predict intra-organ transport as well as inter-organ transport; in every organ, additional rate constants must be introduced to describe how the NPs are transported from the vascular lumen to the extravascular tissue and phagocytic compartments ($k_{tiss\text{-}phago}$, $k_{vasc\text{-}tiss}$, and $k_{vasc\text{-}phago}$ in Fig. 2B). In this case it is assumed that the phagocytes do not change their location within the body after taking up the NPs. Though it is established that macrophages will phagocytose

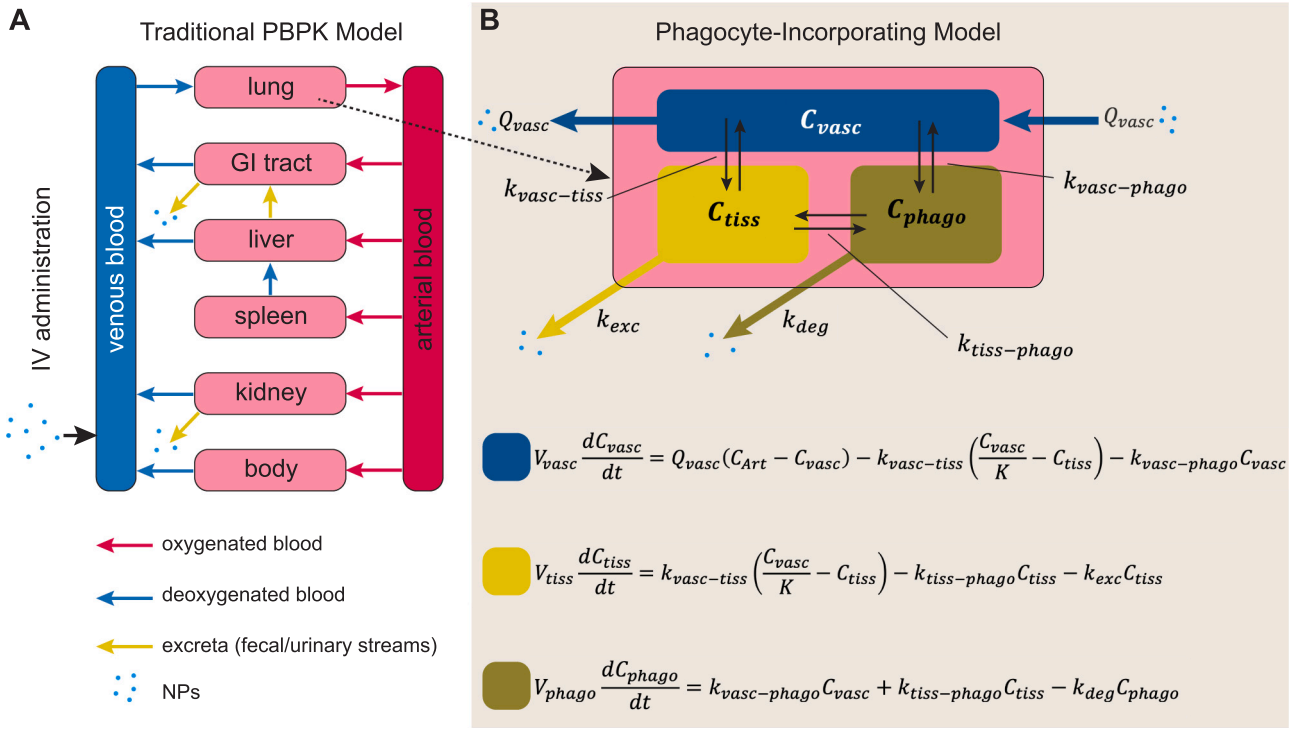

Fig. 2. PBPK model structures. (A) Traditional PBPK model of NP circulation throughout the organ compartments of the body. (B) Phagocyte-incorporating models assume an intravascular, extravascular and phagocytic sub-compartment in each organ. As a result, there are more rate constants that describe the transport of NPs between compartments (denoted $k_{vasc\text{-}tiss}$, $k_{vasc\text{-}phago}$, $k_{tiss\text{-}phago}$), and clearance from the organ by excretion (k_{exc}) and phagocytic degradation (k_{deg}). Subscripts phago, tiss, and vasc denote phagocytic, tissue and vascular sub-compartments. C and V denote NP concentration and organ volume, respectively, with Q_{vasc} denoting the blood flow through the organ. K is defined as in Eq. (3), to denote the ratio of intravascular and extravascular NP concentration. For the intents of this figure, it is assumed that the uptake of NPs into the extravascular space is a membrane-limited process whereas phagocytic uptake of NPs is assumed dependent on the intravascular and/or extravascular NP concentrations alone.

inorganic NPs and carry them to other parts of the body [60], this phenomenon has not been established in polymeric NPs.

The set of NP transport rate constants ('PBPK parameters') are often dependent on NP characteristics [7,59], route of administration [61], and disease state [62]. One of the most straightforward forms of rational NP design involves the optimization of PBPK parameters through quantitative structure-activity relationships (QSAR) [61,63–65]. In general, QSAR is a methodology by which the structure of a drug (small molecule, biologic, nanocarrier, *etc.*) is quantitatively mapped to the drug's pharmacokinetic and/or pharmacodynamic behavior. For pharmacokinetics, this is usually performed by constructing a statistical model that calculates the drug's uptake in different organ compartments as a function of the drug's chemical structure. In NP QSAR, pharmacokinetic and biodistribution data are used to statistically model the dependence of PBPK parameters on NP characteristics, which is often assumed to be linear. To accurately develop robust polymeric NP QSAR, experimental pharmacokinetics data pertaining to different polymeric NPs must be gathered and modeled using PBPK.

A few studies have used PBPK modeling to analyze the pharmacokinetic properties of polymeric NPs. Generally, the NP characteristics tested in these studies include NP size, zeta potential and surface PEG content, which have differential effects on the NP uptake rates in each organ. Each NP characteristic does not uniformly correlate with particular pharmacokinetic properties. For example, the PEG/mPEG content is positively correlated with liver NP uptake for PLGA and polyacrylamide (PAA) NPs [7,66], negatively correlated with liver uptake for PCL NPs [67], and uncorrelated with liver uptake for PLA NPs [68]. When PEGylated, PAA shows a reduced accumulation in the lung [66], while PLGA shows an *increased* accumulation in the lung [68]. These differences suggest that the base, or core, polymer influences the relationship between surface PEG content and NP biodistribution.

In PBPK studies by Li et al. [69], multiple polymeric NP formulations (PAA, PLGA, and PLA) were compared in terms of their rate of phagocytic uptake $k_{tiss\text{-}phago}$ in a phagocytic PBPK model. PAA had the highest rate of phagocytic uptake ($k_{tiss\text{-}phago} \sim 10$), while PLGA had the lowest rate of phagocytic uptake ($k_{tiss\text{-}phago} \sim 0.1$). Even with PEGylation, the $k_{tiss\text{-}phago}$ of PAA was still ~100 times greater than that of PLGA. This indicates that the NP polymer backbone has its own effect on how NPs interact with phagocytes, and PEGylation of different polymer backbones may meagerly tune that interaction. However, this theory cannot be corroborated without further experimental and PBPK modeling studies, as the PAA and PLGA NPs in the study by Li et al. were of different sizes: 31 nm diameter for PAA and 110 nm diameter for PLGA. NP size can also modulate NP-phagocyte interactions, thus comparing the NPs on the exclusive basis of their material composition may lead to erroneous conclusions. It is apparent that, when comparing the results of multiple polymeric NP PBPK studies, it is difficult to directly correlate a change in one NP characteristic to a change in that NP's pharmacokinetics, as there are too many confounding factors. Furthermore, synchronizing different measurement protocols, such as ICP-AES and fluorescence imaging, risks inaccuracy and/or uncertainty in the experimental data. Development of robust QSAR for predicting NP pharmacokinetics requires a significant volume of NP characterization and pharmacokinetic data, ideally gathered using standardized methods.

One of the primary obstacles to the realization of rational design of polymeric NPs using PBPK models is the certainty of the experimental data used to estimate model parameters. A major source of uncertainty in translating pharmacokinetic data to PBPK model parameters is the inherent uncertainty of fluorescence intensity quantification in judging polymeric NP biodistribution [32]. Without alteration (addition of a heavy metal or radioactive tag [70,71]), polymeric NPs are not imageable by computed tomography (CT), single positron emission computed tomography (SPECT), or positron emission tomography (PET). Therefore, typical strategies for collecting polymeric NP pharmacokinetic and/or biodistribution data rely on loading these NPs with a fluorescent dye and comparing the fluorescence intensities of different organs after NP administration.

LLEQ is the standard method for quantifying NP concentration in mouse organs but requires additional tissue dissolution and dye extraction steps that are experimentally involved. Additionally, plate readers used to measure fluorescence in the extracted dyes are also subject to error (*e.g.* due to liquid level inconsistencies). *Ex vivo* imaging, wherein multiple organs are removed from the animal and imaged at once, is a simple modality for comparing NP biodistribution across organs using fluorescence. However, this modality is prone to vastly overestimating NP concentration in small tissues such as tumors [37]. Fluorescence imaging is prone to saturation, such that the NP concentration in high-fluorescence organs (*e.g.* the liver) will be underestimated. When comparing the fluorescence of an organ to that of the liver, that organ's NP concentration may appear higher, because the liver signal has been saturated [37]. Due to fluorescent quenching, a higher concentration of hydrophobic fluorescent dye in the NPs can result in a reduction in their fluorescence [72]. Additionally, NP fluorescence can de-quench over time, increasing the NP fluorescence at a rate dependent on the (unknown) NP concentration in the tissue [73]. Lastly, the emission of different fluorescent dyes is sensitive to environmental conditions such as water content and pH of the tissue [32], further complicating the issue of quantitatively comparing the fluorescence of organs that differ in their cellular homeostatic conditions.

There have been several technologies proposed to solve the problems mentioned above, so that polymeric NP biodistribution can be quantified without radiolabelling the NP surface. Bertrand et al. [41] incorporated ^{14}C into PLGA to create inherently radioactive (beta emitting) NPs. Li et al. [67] used an environmentally-responsive dye that quenches upon contact with water. This allowed them to estimate the biodistribution of only the intact NPs, essentially by using the fluorescence quenching effect to their advantage [74]. This strategy is particularly effective at reducing the fluorescence of dye released in the circulation as the NP polymeric shell degrades [42], a common source of noise in NP pharmacokinetic studies. Lastly, a novel method of quantifying polymeric NP uptake in tissues involves the use of matrix-assisted laser desorption/ionization; here, attachment of alkali metal ions to PEG dendrons and tandem mass spectrometry can quantify polymers based on their structures alone [75]. This method, though exciting, requires the development of specialized encoded polymers and thus may limit the properties of the resulting NPs.

4. Multiscale mathematical modeling of *in vivo* NP delivery

While PBPK models are excellent tools for interpreting NP pharmacokinetic and biodistribution data in animal models, PBPK models cannot effectually recapitulate the complex, multiscale behaviors of NPs (Fig. 3). A PBPK model may inform us about how NPs accumulate in organs but cannot provide a mechanistic understanding of *why* NPs accumulate differently depending on their characteristics. Multiscale mathematical modeling of NP delivery considers NP transport at all relevant scales, from the systems scale (PBPK models) to the nanoscale (cell membrane-NP interaction models) [76–81]. Through multiscale modeling, the behavior of different NP formulations can be predicted from first principles, providing additional information and predictive capabilities. In this context, 'first principles' include the biophysics of NP behaviors at multiple scales; as opposed to PBPK modeling which generalizes NP uptake to individual rate constants that do not necessarily reflect the physics of NP transport, multiscale modeling provides an in-depth view of NP transport by starting with physical principles. We review salient examples of NP modeling at multiple scales and discuss the challenges of implementing multiscale modeling approaches in rational NP design.

At the nanoscale, NPs make contact with the cell membrane and are internalized in cells at different rates depending on the NP characteristics and the cell type. Fundamental models of NP-cell interactions use

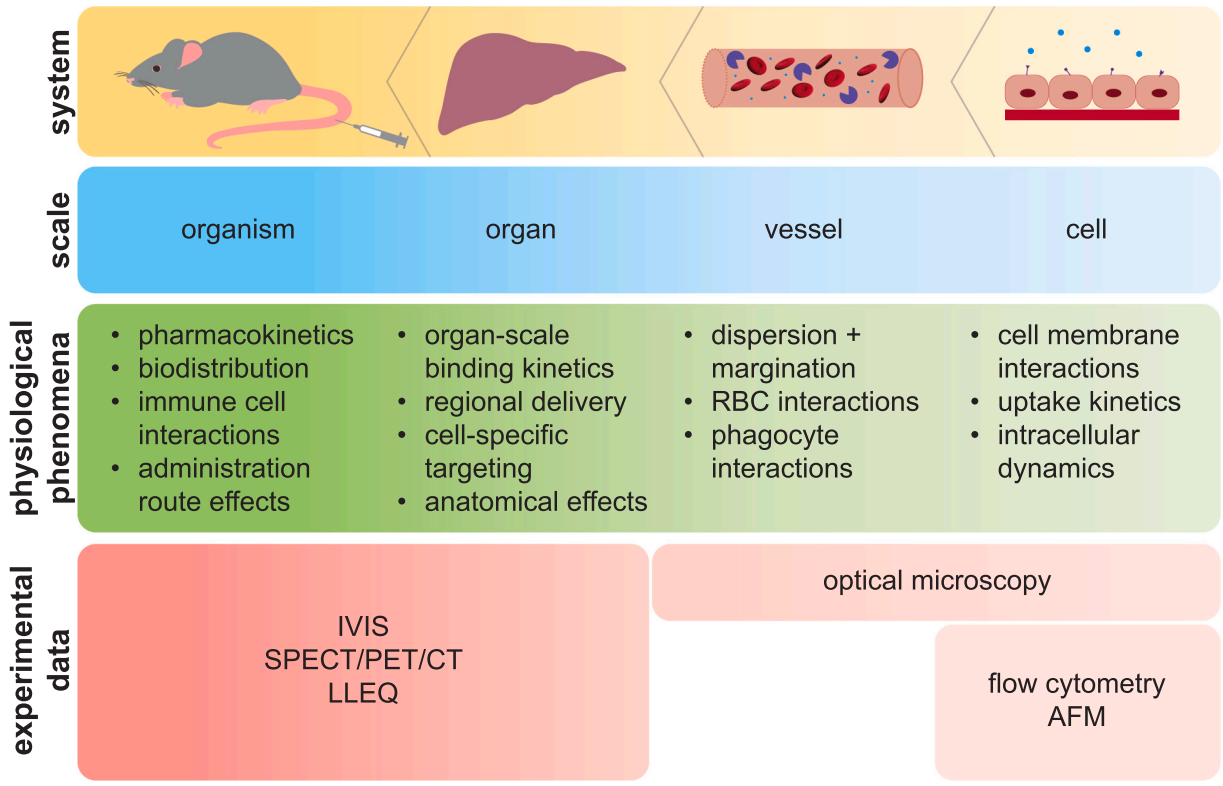

Fig. 3. Multiscale phenomena of NP transport in the body. NPs show distinct behaviors at each scale of the biological system under evaluation: whole-body, organ, blood vessels, and cells. The data required to effectively model these phenomena can be gathered using different methods including flow cytometry, fluorescence quantification, and atomic force microscopy, among others.

systems of ordinary differential equations to describe changes in NP concentration across the cell membrane [82]. These models can be parameterized with data from *in vitro* microscopy studies of fluorescent NPs. Other salient issues in modeling NP-cell interactions are the impact of NP characteristics on their rate of internalization, and the impact of blood flow on NP binding. Modeling studies of NP adhesion and internalization in cells under shear flow have incorporated a geometric component, such that NP size, shape, and surface ligand density affect the rate of adhesion of the NP to the cell surface [83,84]. In these models, the shear rate of blood flow at the vessel wall is incorporated into the calculation of the probability of adhesion to the vessel wall. Similarly, the dislodging of NPs is assumed to occur when the force of NP-cell adhesion (modeled as a flexible ligand-receptor connection) is less than the force exerted on the NP by the flow. These studies suggest that the blood flow at the wall and the rigidity of the NP surface ligands are more important than the affinity of those ligands for the cell surface; a lower compliance of the ligands resulted in significantly better binding, while ligand affinity had less influence on NP adhesion.

While our laboratory and others have shown the benefits of targeting endothelial cells with antibodies conjugated to the NP surface [13–15], non-protein ligands (*e.g.* ACUPA) have been used to selectively target cell receptors (*i.e.* PSMA on prostate cancer cells) [23]. The mathematical models described above can be used to compute the optimal properties of surface ligands for the improvement of cell internalization of NPs under flow, as opposed to solely relying on antibody affinity to determine the NP binding and internalization efficiency.

The models mentioned previously are both useful and simplified; they do not consider the dynamics of multiple NPs as they make contact with the cell membrane, and the membrane itself is assumed flat and static, with a set number of receptors with which NP surface ligands can interact. Alternately, molecular dynamics models consider the dynamics of multiple NPs in three dimensions as they interact with each other and a dynamic cell membrane [85]. This form of modeling is routinely used to investigate antibody-membrane interactions [86], in which the binding affinity of antibodies to the cell surface ligand is quantified as Gibbs free energy [87]. In these simulations, it is possible to model mechanical and molecular factors of the cell membrane that may influence NP adhesion, including the presence of a glycocalyx, membrane curvature, and the flexural rigidity of surface receptors [88]. For example, in the molecular dynamics study by Ramakrishnan et al. [89], it was shown that the flexibility of the cell membrane plays a crucial role in determining NP-cell interactions and adhesion. This result is directly applicable to the context of drug delivery, as cells may have altered membrane mechanical properties depending on their disease state [88]. These studies highlight the importance of characterizing physiological and pathophysiological aspects of drug delivery; even at the cellular scale, physiological processes, such as plasma membrane maintenance, structure, and activity are affected both by cell type and disease processes. These model results indicate the importance of such factors in NP-cell interactions, in addition to the NP characteristics themselves.

At the scale of the lumen of a single blood vessel, NP transport is subject to both the fluid forces of blood flow as well as the Brownian motion characteristics of small particles in fluid (Fig. 4). Tan et al. [90] modeled NP concentration as a continuum, advected by blood flow, diffusing towards the vessel wall. At the site of the wall, a second model incorporated Brownian dynamics to simulate NP stochastic movement, and a ligand-binding model was used to simulate NP-cell adhesion. This 'model coupling' is the main strategy by which multiscale models represent the very different physical effects associated with each length scale (diffusion, advection, Brownian motion, wall-binding). Vessel models can also incorporate the dynamics of flexible red blood cells (RBCs), which alter the flow and can impact NP margination towards the wall. Muller et al. [91] modeled RBC-NP interactions in cylindrical vessels under shear flow, and found that there is an optimal concentration of RBCs to disperse NPs towards the vessel wall; higher hematocrit can lead to NPs collecting in the center due to fluid drag from the

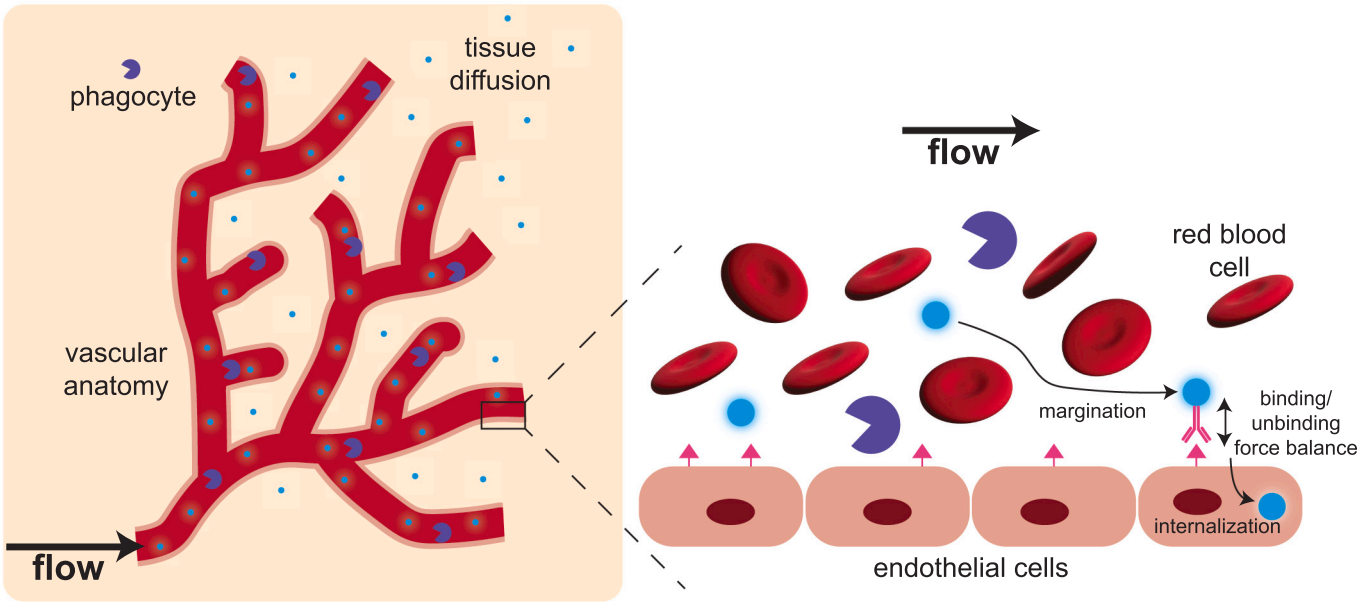

Fig. 4. NP transport in vascular systems is typically modeled as a continuum that distributes throughout the vascular anatomy (left). Intraluminally, NPs interact with phagocytes and red blood cells before marginating to the wall and binding to the endothelial cells (right). Typical models of NP-cell interaction model the force balance between the NP's binding to the cell surface and the hemodynamic force that drives the NP away from the wall. (For interpretation of the references to colour in this figure legend, the reader is referred to the web version of this article.)

blood cells, while a lower hematocrit results in NPs marginating to the uninhabited vessel center. Thus, an intermediate hematocrit is optimal for NP dispersion towards the wall, a result replicated by Fullstone et al. [92]. Cooley et al. [93] used a vessel model of NP dispersion in a capillary to estimate the impact of NP size and shape on their dispersion towards the wall, and showed that a larger particle size and oblate shape produced the highest dispersion and contact with the wall.

Intraluminal NP transport models such as those discussed above provide nuance to the fundamental issue of NP margination under flow; factors that influence NP-wall interaction frequency include hematocrit, vessel geometry, and NP size and shape, as these variables impact NP motion both far from and near the vessel wall. From a drug delivery standpoint, these results indicate that estimating NP delivery at the scale of vessel networks requires modeling schema that account for variance in these parameters across vessel segments. For example, the vessel segments of a glomerulus vary significantly in terms of their geometry, flow, shear rate, hematocrit, and filtration rate [94,95]. Individual vessel models provide an understanding of how these factors influence NP transport and may provide a means to estimate how NP transport varies across entire networks of blood vessels as a result of this heterogeneity.

At the scale of blood vessel networks and organs, NPs are again modeled as a continuum advected by blood flow (Fig. 4). Using CT images of patient carotid arteries, Hossain et al. [96] modeled drug-encapsulated NP transport through the arterial lumen and into the artery wall. After making contact with the wall, the NPs diffuse into the tissue composed of adventitia and intima. Particulate diffusion models have been used to estimate NP penetration into various tissues [97] and can serve as a coupled model in the greater arterial network modeling scheme to estimate drug delivery to atherosclerotic plaques [96]. A similar scheme was utilized by Sohrabi et al. to study the transport dynamics of NPs in patient-specific pulmonary arterial networks [24,98]. In this case, the NPs were modeled as rigid particles with both Brownian and fluidic motion, and a binding probability function was used to estimate the stochastic nature of NP-wall adhesion. Li et al. [99] developed a multiscale computational model of NP transport in patient-specific arterial networks which included RBC-NP interactions, NP-wall interactions, and a model of endosomal rupture of the NPs inside the target cell. These studies clearly show the utility of model coupling in representing NP transport at multiple scales and the 'personalization' of these models by incorporating patient-specific anatomical features.

Another salient form of modeling NP transport at the organ scale involves modeling NP transport through tumor tissues [81]. Frieboes et al. [100] modeled anti-angiogenic drug-encapsulating NP transport through a dynamic tumor model with blood vessels that changed in density and location over time. These studies indicated that the vascularity of the tumor plays a crucial role in NP transport, and that in the event of low tumor vascularity, NPs will preferentially flow into healthy vessels that will bypass the tumor. This effect plays an important role for anti-angiogenic drugs, in which the therapy itself reduces the vascularity of the tumor and thus the transport of drug-encapsulated NPs [101]. Further studies from this group investigated the effects of alterations in NP characteristics on NP transport in cancer tissue, showing that NP diameter and avidity as well as drug potency can be effectively optimized for reducing tumor diameter [102,103]. Goodman et al. [104] used a mathematical model of fluorescent NP penetration into cancer spheroids, and showed that adding collagenase to the spheroid media increased the porosity of the spheroid and increased NP penetration depth.

The value of multiscale modeling of NP transport in the body is the ability to model many physical phenomena simultaneously, which may result in the discovery of unexpected behaviors that a PBPK model will not capture. PBPK models can recapitulate the gross behaviors of NPs in terms of their distribution to different organs and tissues but cannot show how a NP interacts with different cell types in a tissue, or how the NP is transported in capillary networks. As a result, there are NP formulations that appear to target tissues effectively according to PBPK models, but do not reach the target cells within the organs due to some physical effect not captured by PBPK models. By developing a fully multiscale framework, the characteristics of the NP and the biological milieu can be modeled and used to optimize the NP formulation for a particular drug delivery application.

Multiscale models of NP delivery face substantial challenges in their ability to predict NP behavior. First, multiscale modeling is naturally hindered by computational cost; modeling NP transport at all scales simultaneously requires prohibitively expensive computational

resources and time to perform these costly simulations. Instead, multiscale models of NP transport typically couple multiple models together; each scale (whole body, organs, vessels, cells) are modeled separately, and these models are interfaced to predict how cell-scale NP transport properties impact NP transport at the scale of organs and organ systems [99]. The challenge with this modeling strategy is the potential for compounding error; as one model's output becomes the input for another model of the next relevant scale, the inaccuracy of the first model is passed on to the second, with the potential to drastically alter the end result [105]. Several computational approaches have been used to control the error between models at different scales; for example, Prudhomme et al. used an adaptive method of coupling atomistic and continuum models wherein the error is minimized through the coupling scheme [106].

To reduce the risk of compounding error between sub-models, previous multiscale modeling studies parameterized and validated each sub-model with separate experimental datasets. Liu et al. [107] developed a model of an ICAM-1 antibody-conjugated NP interacting with an endothelial cell membrane using atomic force microscopy (AFM) data. AFM has been used extensively to quantify the strength of NP-membrane binding with different NP surface functionalization (*e.g.* antibody conjugation) [108–114]. Interestingly, Liu et al. found that, for securing NPs to the cell membrane, the affinity of the NP surface antibody for ICAM-1 played a less important role than multivalency wherein multiple antibody-antigen connections immobilized the NP and improved its adhesion to the cell. At the vessel scale, Van de Ven et al. [115] used intravital microscopy of mouse tumors to parameterize the previously-discussed model of NP transport in vascularized tumor tissue [100]. Thus, there are several experimental modalities that will provide data appropriate for parameterizing individual sub-models in a multiscale modeling schema.

Another crucial challenge—in the effort to model NP delivery at multiple scales—is the challenge of model validation. Ultimately, the proving ground for a NP formulation is an *in vivo* model, wherein the NPs will traverse all relevant scales in their path to their target(s). A key advantage of *in vivo* models is their accurate representation of anatomy and physiology, both of which play an important role in NP transport. However, small animal models are known to differ in their anatomy and physiology from humans; compared to humans, mice and rats have higher heart rates, smaller blood volume, and smaller organs, all of which impact NP pharmacokinetics [116]. Even at the microvascular level, humans show distinct differences from mice and rats; unlike rodent glomeruli, human glomeruli have non-filtering 'chambers' in addition to the usual filtering capillaries, which is hypothesized to differentiate human glomerular hydrodynamics from that of mice and rats [117]. Large animal models (*e.g.* pigs, sheep, non-human primates) are much more expensive than small animals and fail to capture the substantial anatomical variability of the human population. Disease animal models can introduce additional discrepancies. To address this problem, we have used *ex vivo* normothermic machine-perfused human organs to evaluate the targeting efficacy of antibody-conjugated PLA-PEG NPs [13–15,36]. Though difficult to execute, this experimental setup is ideal for characterizing the transport of NPs in human organs and has the potential to aid in the development of increasingly sophisticated models of NP transport. To experimentally model NP transport at the vessel scale, we have used isolated perfused human umbilical veins [118] and microfluidic systems [13], both of which are useful in the characterization of NP dispersion and cell interactions under flow.

5. The future of NP pharmacokinetic optimization

The lofty goal of rational polymeric NP design presents two fundamental challenges to mathematical models: (1) the human physiological processes relevant to NP pharmacokinetics—such as the dynamics of the cardiovascular and immune systems—are difficult to recapitulate in computational models; and (2) the multiscale behaviors of NPs are difficult to quantitatively map to particular NP characteristics due to experimental uncertainty. Experimental uncertainty in NP pharmacokinetics studies is due to the methodologies themselves (*i.e.* NP fluorescence intensity quantification), as well as the time and resource challenges that make it difficult to produce the high-throughput NP pharmacokinetic data needed to effectively validate NP transport models. Meta-analysis models that integrate multiple datasets into one modeling framework present the opportunity to parameterize models based on comprehensive, multicenter datasets and not individual, siloed datasets. Cheng et al. [63] integrated 200 NP pharmacokinetic datasets, spanning myriad NP types and surface properties, to model each case with the same PBPK model. By parameterizing the model with these different datasets, it was possible to compare pharmacokinetic parameters between groups of NPs with different characteristics, the crucial first step towards rational NP design. Although this effort did not take the next step to develop QSAR between NP characteristics and their pharmacokinetics, the integration of multiple datasets could theoretically reduce the uncertainty of the model results. In future studies, rigorous validation will be required to determine if the error generated by a single dataset is reduced as more datasets are incorporated.

Another mathematical modeling technique uses Bayesian statistics to incorporate experimental uncertainty into the model construction. Practically, this approach involves parameterizing and validating the model based on experimental data represented by a distribution with mean and standard deviations (how experimental data is presented) as opposed to a single number. Thus, model accuracy is quantifiable as a function of the error in the data used to parameterize and/or validate the model. Chou et al. [61] used a Bayesian PBPK modeling framework to integrate multiple pharmacokinetic datasets corresponding to differently-sized gold NPs administered orally, intravenously, intratracheally, and endotracheally. This study showed that the administration route played a greater role in determining biodistribution patterns than the NP characteristics. Due to the Bayesian nature of the modeling framework, parameters and model results were represented as probability distributions. Practically, this means that it is readily apparent how well the model fits the data, and how confident we can be that the model results reflect reality and are not based solely on potentially erroneous datapoints. Furthermore, by representing model outputs as probability distributions, a Bayesian model shows how confident we can be in a particular model result.

The other crucial benefit to a Bayesian modeling framework is that more data can be incorporated into the framework over time; an initial dataset can be used to construct the parameter distributions that predict NP pharmacokinetics based on their general properties (such as material, charge, size, surface PEG content), then additional, specialized data can be incorporated to specify the NP characteristics for a particular disease state or target cell type. This approach could be useful for generating hypotheses to test experimentally, to better predict the effect of a specific NP characteristic on its pharmacokinetic behavior; further, this feature could be applied to incorporate human anatomical and/or physiological variability into the modeling pipeline.

From multiscale modeling, it is apparent that physiology and the target microenvironment play a role of equal importance to NP characteristics in determining NP behavior in the body. Sykes et al. [11] used mouse tumor models of varied size to show that tumor characteristics (size, vascularity, cell type) directly impact NP delivery. Dos Reis et al. [119] showed that the age of the animal impacts NP delivery. From a pathophysiological standpoint, changes in liver, spleen and/or kidney function due to disease will naturally affect NP clearance and circulation. These factors motivate the potential need for 'personalized nanomedicine,' wherein NPs are designed on the basis of the anatomy and physiology of individual patients. Taken to the extreme, Lazarovits et al. [120] developed patient-derived protein-based NPs for patient-specific drug delivery.

Polymeric NPs themselves show variability in their properties depending on their formulation protocol. Depending on the method

used (nanoprecipitation, single or double emulsion and solvent evaporation, *etc.*) the material and formulation parameters (polymer composition, molecular weight, agitation speed, temperature) can influence the NP size, zeta potential and surface characteristics [121]. Quality by Design (QbD) is a methodology frequently employed in drug development, involving the optimization of chemical synthesis by screening different factors that may alter the chemical's properties. In the case of NPs, QbD has recently been used to screen for the material/formulation protocol parameters that may influence the NP's properties, and then optimize those parameters to produce precisely-tuned NPs [122]. This methodology also involves design of experiments (DoE), a statistical methodology whereby the optimal amount of information is gleaned from the minimal amount of experiments. Although the QbD process is similar to QSAR, QbD is more focused on the quality and reproducibility of NP formulation. Thus, the combination of QbD and QSAR will ultimately allow for a comprehensive predictive pipeline to design the production of NPs that have the desired pharmacokinetic profile for a particular drug delivery application. QbD can be incorporated into a Bayesian framework as well, such that the ultimate model pharmacokinetic prediction is based on the NP formulation parameters and not just the NP characteristics alone.

There is a wealth of data describing the pharmacokinetics of NPs that can be mined to optimize NP formulations for particular applications. However, the true challenge in NP design optimization is determining how to integrate these data to make valid predictions [123]. To robustly predict the optimal NP formulation, it appears necessary to combine multiple datasets that examine different NP characteristics and their influence on NP pharmacokinetics [63]. In this case, a robust prediction has both: (1) low uncertainty and (2) accounting of the multiscale nature of NP behavior.

A helpful conceptual tool for visualizing NP formulation optimization is a quantitative NP design framework (Fig. 5). In this example, raw materials are converted to NPs through formulation techniques that can be optimized using QbD to create NPs with reproducible physicochemical characteristics. These NPs are tested in experimental settings, and the results of these experiments are used to either parameterize a multiscale model of NP delivery or validate its results. The set of model parameters that emerges from the parameterization of the model based on experimental data (Fig. 5, arrow in green) describe NP behavior at multiple scales and can be quantitatively mapped to the NP characteristics using statistical models (QSAR). Finally, for a particular drug delivery application, the multiscale model can be used to estimate which model parameters will optimize NP targeting efficiency. Through QSAR and QbD, those model parameters are mapped back to a plan for NP formulation. The multiscale model developed through the framework can also simulate how a particular NP type will behave in the body at all relevant scales, which is useful for reducing costly NP pharmacokinetics experiments.

Another advantage to NP design frameworks is that they define a set of standardized data analysis, models and parameterization schema that ensure that all NP characteristics can be accurately compared. This is useful because results of individual experimental studies are difficult to compare; as stated earlier, the influence of one NP characteristic on its pharmacokinetics is difficult to judge due to the confounding factors of other NP characteristics, and it is unlikely that two studies will have the exact same NPs that differ in only one characteristic. Modeling studies are difficult to compare if the model structures are different. In the quantitative NP design framework described in Fig. 5, different data are incorporated into the parameterization of one standard (potentially multiscale) model. In the end, the raw data pertaining to a study of one NP formulation may not be comparable to the raw data of that of another formulation, but the two formulations can be compared in terms of their model parameters that are standardized across all experimental cases included in the design framework.

This viewpoint has some basis: quantitative NP design frameworks have been explored for non-polymeric NP systems. Dogra et al. [64]

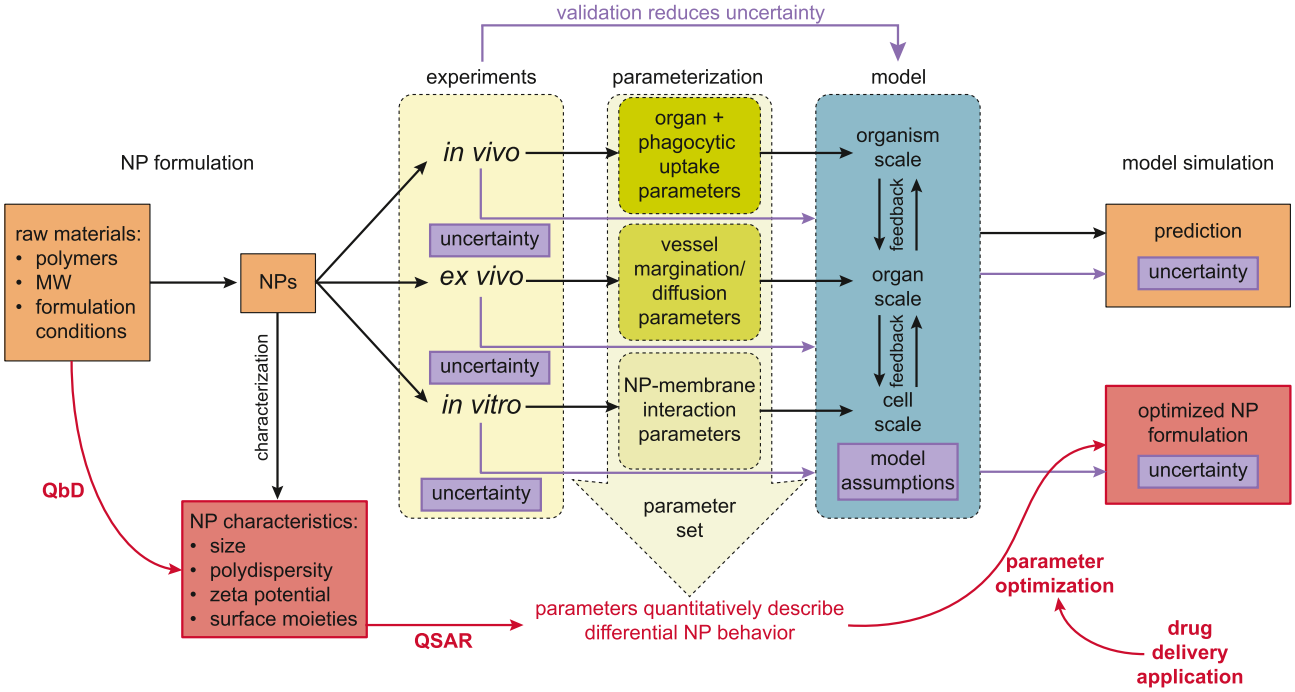

Fig. 5. A generalized quantitative NP design framework. Raw materials are combined to formulate a NP, which is used in experiments that characterize that NP's behavior at multiple scales. A parameterizations schema (green) is used to convert that experimental data into parameters for a multiscale model of NP transport (blue). That model can then either produce simulations of how a given NP formulation will behave in the body or be used to optimize the NP formulation for a particular drug delivery application (red). QSAR and QbD are used to map NP characteristics to model parameters and NP formulation parameters to the NP characteristics, respectively. Uncertainty in experimental data (purple), propagates to model assumptions and can introduce error or uncertainty into model results. Validation of the model using experimental data helps to reduce model uncertainty.

developed a multiscale PBPK model of silica NP delivery to rat tumors. This model was parameterized with data from silica NPs of varied size (45 nm to 160 nm in diameter) and was extensive in its representation of physiological processes at multiple scales; an overall PBPK model was used to model NP transport between organs, and organs had intravascular, extravascular and phagocytic sub-compartments (as in Fig. 2B). Within each sub-compartment, a separate set of equations described the micron-scale NP dynamics involving vessel margination and wall adhesion (intravascular sub-compartment), as well as cell-scale phenomena such as NP internalization and phagocytosis (phagocytic sub-compartment). The data used to generate the overarching PBPK model were gathered in a former study using SPECT/CT images of indium-labelled mesoporous silica NP biodistribution in rats [124]. This combination of NP imaging with mathematical modeling of NP pharmacokinetics creates a quantitative NP design framework; NPs with varied characteristics go through a pipeline of experiments, parameterization, and model construction, to ultimately predict how they will vary in their biodistribution based on their characteristics. This imaging-modeling pipeline is reviewed by Dogra et al. in detail elsewhere [125].

These studies showed how a quantitative NP design framework can be constructed, with imaging data used to parameterize a PBPK model of NP transport. With parametric sensitivity analyses, they showed that multiple pharmacokinetic parameters are sensitive to NP characteristic manipulation; the NP radius, density and degradation rate had significant impact on tumor accumulation and excretion, for example. However, they did not take the additional step of optimizing the NP formulation to target tumor tissue. The Bayesian PBPK model framework developed by Chou et al. [61] is another example of the basic structure of a quantitative NP design framework, in that gold NPs with different characteristics were modeled by parameterizing a PBPK model with pharmacokinetics data from rats. The mathematical model is also Bayesian, such that additional data can be incorporated over time. To our knowledge, this platform has not yet been implemented to optimize NPs for a particular drug delivery application.

The modeling studies above highlight the interest in modeling NP pharmacokinetics as a function of the NP characteristics, but such a strategy has not been employed to comprehensively model polymeric NP pharmacokinetics. At the most basic level, polymeric NPs usually have lower density and higher polydispersity than inorganic NPs. Both of these factors influence experimental results as well as modeling schema. For example, modeling NPs with a distribution of sizes may require Monte-Carlo and/or Bayesian methods to account for the differences in NP behavior associated with that polydispersity. The future of polymeric NP optimization will rely on the development of appropriate mathematical models that can be used to integrate many polymeric NP pharmacokinetic datasets.

6. Conclusion

Polymeric NPs present the opportunity to create a wide array of nanocarriers with different combinations of physicochemical attributes. Rational NP design is a strategy by which mathematical models are used to optimize these characteristics for specific drug delivery applications. The optimal modeling approach for realizing rational NP design must allow for the integration of many different experimental datasets to fully map the design space of polymeric NPs. Studies that use individual datasets provide distinct insights into how a particular NP characteristic influences its pharmacokinetics [7], but it is difficult to extrapolate these results to NPs with different core materials, surface alterations, and size. Here, we present the concept of a quantitative NP design framework, which could provide a pipeline for many pharmacokinetic datasets to be incorporated into one model *via* parameterization of the model or validation of the model's results. By using a standardized model, it should be possible to combine this data to generate more robust predictions.

To integrate multiple NP pharmacokinetics datasets into one model, it is essential to understand that there are diverse methodologies for measuring NP uptake in organs and cells, each with their advantages and disadvantages. In particular, fluorescence intensity quantification is prone to several errors and uncertainties that will propagate to the model results [32]. Fluorescence is relative and fluorescence saturation, quenching and de-quenching are bound to affect model results [37]. Nuclear imaging modalities may be useful for validating fluorescence quantification data before they are used to parameterize or validate the mathematical model. Multiscale modeling of NP delivery presents the opportunity to predict complex or nonlinear NP pharmacokinetic behavior, thus multiscale models are preferable to PBPK models alone. Multiscale modeling also provides the opportunity to incorporate more mechanistic, experimental data of NP-cell interactions obtained by AFM, flow cytometry, and quantitative microscopy. A key challenge in multiscale modeling is validation of the model. We believe that *ex vivo* human organ perfusion provides a unique, controlled experimental system to test particular hypotheses generated by a multiscale model of NP delivery in human organs [14,126].

Taking a broad view of the field of nanomaterial-based drug delivery, there has been an emphasis on obtaining a 'magic bullet:' a modality that directs the vast majority of drug to a single cell type, tissue, or anatomical niche [123]. In reality, the 'magic bullet' for any tissue type has yet to be discovered; current NP-based drug delivery methods, though they may improve targeting of the loaded drug, still produce modest gains in the face of off-target accumulation [127]. This sobering point shows that there are great strides to be made in the field of nanomedicine. Notably, this also indicates that the methodologies we have used – involving siloed experiments and modeling studies to empirically predict which NPs will be optimal for a particular drug delivery application – are not adequate to produce generalizable results. Instead, we posit that large volumes of data must be integrated to adequately cover the polymeric NP design space, and that one standard mathematical model must be used to compare NP formulations to ultimately decide the optimal formulation for a particular drug delivery application.

CRediT authorship contribution statement

Owen Richfield: Writing – original draft, Writing – review & editing. **Alexandra S. Piotrowski-Daspit:** Visualization, Writing – original draft, Writing – review & editing. **Kwangsoo Shin:** Writing – original draft, Writing – review & editing. **W. Mark Saltzman:** Funding acquisition, Writing – original draft, Writing – review & editing.

Data availability

No data was used for the research described in the article.

Acknowledgements

Our original work in this field is supported by grants from the National Institutes of Health: AI32895, HL147352, and CA149128. O.R. is supported by an NIH NRSA (5T32DK007276). A.S.P. is supported by a K99/R00 Pathway to Independence award from the NIH (K99 HL151806) and a Postdoc-to-Faculty Transition Award from the Cystic Fibrosis Foundation (CFF; PIOTRO21F5).

We dedicate this paper to Professor Kinam Park, who is a pioneer in drug delivery technology and, more importantly, a truth-teller in inspiring the field to think in a rational way about the advantages of advanced technologies for drug delivery, particularly nanoparticle-based approaches. We are grateful to Professor Park for his years of dedicated service as Editor-in-Chief at the Journal of Controlled Release, where he lead the JCR team with wisdom, rigor, and fairness. One of us (W.M.S.) is particularly grateful to Professor Park for his kindness over these many years.

References

[1] B. Pelaz, et al., Diverse applications of nanomedicine, ACS Nano 11 (3) (2017) 2313–2381.
[2] M.E. Gindy, R.K. Prud'homme, Multifunctional nanoparticles for imaging, delivery and targeting in cancer therapy, Expert Opin. Drug Deliv. 6 (8) (2009) 865–878.
[3] A.C. Anselmo, S. Mitragotri, Nanoparticles in the clinic: an update, Bioeng. Transl. Med. 4 (3) (2019), e10143.
[4] H. Park, A. Otte, K. Park, Evolution of drug delivery systems: from 1950 to 2020 and beyond, J. Control. Release 342 (2022) 53–65.
[5] R.F. Pagels, R.K. Prud'homme, Polymeric nanoparticles and microparticles for the delivery of peptides, biologics, and soluble therapeutics, J. Control. Release 219 (2015) 519–535.
[6] B. Begines, et al., Polymeric nanoparticles for drug delivery: recent developments and future prospects, Nanomaterials 10 (7) (2020) 1403.
[7] M. Li, et al., Physiologically based pharmacokinetic modeling of PLGA nanoparticles with varied mPEG content, Int. J. Nanomedicine (2012) 1345–1356.
[8] A.C. Kauffman, et al., Tunability of biodegradable poly (amine-co-ester) polymers for customized nucleic acid delivery and other biomedical applications, Biomacromolecules 19 (9) (2018) 3861–3873.
[9] J. Liu, et al., Simple and tunable surface coatings via polydopamine for modulating pharmacokinetics, cell uptake and biodistribution of polymeric nanoparticles, RSC Adv. 7 (26) (2017) 15864–15876.
[10] S. Kim, et al., Engineered polymers for advanced drug delivery, Eur. J. Pharm. Biopharm. 71 (3) (2009) 420–430.
[11] E.A. Sykes, et al., Tailoring nanoparticle designs to target cancer based on tumor pathophysiology, Proc. Natl. Acad. Sci. 113 (9) (2016) E1142–E1151.
[12] M. Sethi, et al., Effect of drug release kinetics on nanoparticle therapeutic efficacy and toxicity, Nanoscale 6 (4) (2014) 2321–2327.
[13] C. Albert, et al., Monobody adapter for functional antibody display on nanoparticles for adaptable targeted delivery applications, Nat. Commun. 13 (1) (2022) 5998.
[14] G.T. Tietjen, et al., Nanoparticle targeting to the endothelium during normothermic machine perfusion of human kidneys, Sci. Transl. Med. 9 (418) (2017) eaam6764.
[15] J.R. DiRito, et al., Lysis of cold-storage-induced microvascular obstructions for ex vivo revitalization of marginal human kidneys, Am. J. Transplant. 21 (1) (2021) 161–173.
[16] F. Alexis, et al., Factors affecting the clearance and biodistribution of polymeric nanoparticles, Mol. Pharm. 5 (4) (2008) 505–515.
[17] K. Parmar, J. Patel, Y. Pathak, Factors affecting the clearance and biodistribution of polymeric nanoparticles, in: Pharmacokinetics and Pharmacodynamics of Nanoparticulate Drug Delivery Systems, Springer, 2022, pp. 261–272.
[18] A. Zhang, et al., Absorption, distribution, metabolism, and excretion of nanocarriers in vivo and their influences, Adv. Colloid Interf. Sci. 284 (2020), 102261.
[19] H.T. Ta, et al., The effects of particle size, shape, density and flow characteristics on particle margination to vascular walls in cardiovascular diseases, Expert Opin. Drug Deliv. 15 (1) (2018) 33–45.
[20] R. Toy, et al., The effects of particle size, density and shape on margination of nanoparticles in microcirculation, Nanotechnology 22 (11) (2011), 115101.
[21] A.E. Nel, et al., Understanding biophysicochemical interactions at the nano–bio interface, Nat. Mater. 8 (7) (2009) 543–557.
[22] S.M. Moghimi, A.C. Hunter, T.L. Andresen, Factors controlling nanoparticle pharmacokinetics: an integrated analysis and perspective, Annu. Rev. Pharmacol. Toxicol. 52 (1) (2012) 481–503.
[23] J. Hrkach, et al., Preclinical development and clinical translation of a PSMA-targeted docetaxel nanoparticle with a differentiated pharmacological profile, Sci. Transl. Med. 4 (128) (2012), 128ra39.
[24] S. Sohrabi, et al., Nanoparticle transport and delivery in a heterogeneous pulmonary vasculature, J. Biomech. 50 (2017) 240–247.
[25] S.D. Perrault, et al., Mediating tumor targeting efficiency of nanoparticles through design, Nano Lett. 9 (5) (2009) 1909–1915.
[26] K. Park, Nanotechnology: what it can do for drug delivery, J. Control. Release: Off. J. Control. Release Soc. 120 (1–2) (2007) 1–3.
[27] Y. Chen, et al., Prediction of kidney drug clearance: a comparison of tubular secretory clearance and glomerular filtration rate, J. Am. Soc. Nephrol. 32 (2) (2021).
[28] K.M. Tsoi, et al., Mechanism of hard-nanomaterial clearance by the liver, Nat. Mater. 15 (11) (2016) 1212–1221.
[29] R. Gebhardt, et al., New hepatocyte in vitro systems for drug metabolism: metabolic capacity and recommendations for application in basic research and drug development, standard operation procedures, Drug Metab. Rev. 35 (2–3) (2003) 145–213.
[30] Z.P. Lin, et al., Macrophages actively transport nanoparticles in tumors after extravasation, ACS Nano 16 (4) (2022) 6080–6092.
[31] Q. Dai, et al., Quantifying the ligand-coated nanoparticle delivery to cancer cells in solid tumors, ACS Nano 12 (8) (2018) 8423–8435.
[32] J.B. Simonsen, E.B. Kromann, Pitfalls and opportunities in quantitative fluorescence-based nanomedicine studies–a commentary, J. Control. Release 335 (2021) 660–667.
[33] P.M. Perrigue, et al., Degradation of drug delivery nanocarriers and payload release: a review of physical methods for tracing nanocarrier biological fate, Pharmaceutics 13 (6) (2021) 770.
[34] A.S. Piotrowski-Daspit, et al., In vivo correction of cystic fibrosis mediated by PNA nanoparticles, Sci. Adv. 8 (40) (2022) eabo0522.
[35] K. Shin, et al., Polyglycerol and poly (ethylene glycol) exhibit different effects on pharmacokinetics and antibody generation when grafted to nanoparticle surfaces, Biomaterials 287 (2022), 121676.
[36] L.G. Bracaglia, et al., High-throughput quantitative microscopy-based half-life measurements of intravenously injected agents, Proc. Natl. Acad. Sci. 117 (7) (2020) 3502–3508.
[37] F. Meng, et al., Quantitative assessment of nanoparticle biodistribution by fluorescence imaging, revisited, ACS Nano 12 (7) (2018) 6458–6468.
[38] H.C. Fischer, et al., Quantitative detection of engineered nanoparticles in tissues and organs: an investigation of efficacy and linear dynamic ranges using ICP-AES, Nanobiotechnology 3 (2007) 46–54.
[39] M.R. Gill, et al., 111 in-labelled polymeric nanoparticles incorporating a ruthenium-based radiosensitizer for EGFR-targeted combination therapy in oesophageal cancer cells, Nanoscale 10 (22) (2018) 10596–10608.
[40] K. Szigeti, et al., Thallium labeled citrate-coated prussian blue nanoparticles as potential imaging agent, Contrast Media Mol. Imaging 2018 (2018).
[41] N. Bertrand, et al., Mechanistic understanding of in vivo protein corona formation on polymeric nanoparticles and impact on pharmacokinetics, Nat. Commun. 8 (1) (2017) 777.
[42] W.G. Kreyling, et al., In vivo integrity of polymer-coated gold nanoparticles, Nat. Nanotechnol. 10 (7) (2015) 619–623.
[43] S.A. Kulkarni, S.S. Feng, Effects of particle size and surface modification on cellular uptake and biodistribution of polymeric nanoparticles for drug delivery, Pharm. Res. 30 (10) (2013) 2512–2522.
[44] C.H.J. Choi, et al., Targeting kidney mesangium by nanoparticles of defined size, Proc. Natl. Acad. Sci. 108 (16) (2011) 6656–6661.
[45] H.K. Mandl, et al., Optimizing biodegradable nanoparticle size for tissue-specific delivery, J. Control. Release 314 (2019) 92–101.
[46] K. Ogawa, et al., Orthogonal characterization and pharmacokinetic studies of polylactide-polyethyleneglycol polymeric nanoparticles with different physicochemical properties, Int. J. Pharm. 608 (2021), 121120.
[47] S.M. D'Addio, et al., Effects of block copolymer properties on nanocarrier protection from in vivo clearance, J. Control. Release 162 (1) (2012) 208–217.
[48] A. Verma, F. Stellacci, Effect of surface properties on nanoparticle–cell interactions, Small 6 (1) (2010) 12–21.
[49] H. Zhou, et al., Dense and dynamic polyethylene glycol shells cloak nanoparticles from uptake by liver endothelial cells for long blood circulation, ACS Nano 12 (10) (2018) 10130–10141.
[50] J. Grundler, et al., Surface topography of polyethylene glycol shell nanoparticles formed from bottlebrush block copolymers controls interactions with proteins and cells, ACS Nano 15 (10) (2021) 16118–16129.
[51] C.D. Walkey, et al., Nanoparticle size and surface chemistry determine serum protein adsorption and macrophage uptake, J. Am. Chem. Soc. 134 (4) (2012) 2139–2147.
[52] Z.-T. Cao, et al., Protein binding affinity of polymeric nanoparticles as a direct indicator of their pharmacokinetics, ACS Nano 14 (3) (2020) 3563–3575.
[53] A. Narmani, et al., Folic acid functionalized nanoparticles as pharmaceutical carriers in drug delivery systems, Drug Dev. Res. 80 (4) (2019) 404–424.
[54] C. Huang, et al., Folate receptor-mediated renal-targeting nanoplatform for the specific delivery of triptolide to treat renal ischemia/reperfusion injury, ACS Biomater. Sci. Eng. 5 (6) (2019) 2877–2886.
[55] F. Ordikhani, et al., Selective trafficking of light chain-conjugated nanoparticles to the kidney and renal cell carcinoma, Nano Today 35 (2020).
[56] M. Li, et al., Physiologically based pharmacokinetic modeling of nanoparticles, ACS Nano 4 (11) (2010) 6303–6317.
[57] E.O. Kutumova, et al., Physiologically based pharmacokinetic modeling of nanoparticle biodistribution: a review of existing models, simulation software, and data analysis tools, Int. J. Mol. Sci. 23 (20) (2022) 12560.
[58] M. Li, et al., Physiologically based pharmacokinetic (PBPK) modeling of pharmaceutical nanoparticles, AAPS J. 19 (2017) 26–42.
[59] W.M. Saltzman, Drug Delivery: Engineering Principles for Drug Therapy, Oxford University Press, 2001.
[60] X. Ding, et al., Engineering macrophages via nanotechnology and genetic manipulation for cancer therapy, Front. Oncol. (2022) 11.
[61] W.-C. Chou, et al., Development of a multi-route physiologically based pharmacokinetic (PBPK) model for nanomaterials: a comparison between a traditional versus a new route-specific approach using gold nanoparticles in rats, Part. Fibre Toxicol. 19 (1) (2022) 1–19.
[62] S.R.R. Dos Reis, et al., Senescence and the impact on biodistribution of different nanosystems: the discrepancy on tissue deposition of graphene quantum dots, polycaprolactone nanoparticle and magnetic mesoporous silica nanoparticles in young and elder animals, Pharm. Res. 37 (2020) 1–12.
[63] Y.-H. Cheng, et al., Meta-analysis of nanoparticle delivery to tumors using a physiologically based pharmacokinetic modeling and simulation approach, ACS Nano 14 (3) (2020) 3075–3095.
[64] P. Dogra, et al., A mathematical model to predict nanomedicine pharmacokinetics and tumor delivery, Comput. Struct. Biotechnol. J. 18 (2020) 518–531.
[65] Z. Lin, N.A. Monteiro-Riviere, J.E. Riviere, A physiologically based pharmacokinetic model for polyethylene glycol-coated gold nanoparticles of different sizes in adult mice, Nanotoxicology 10 (2) (2016) 162–172.
[66] U. Carlander, et al., Toward a general physiologically-based pharmacokinetic model for intravenously injected nanoparticles, Int. J. Nanomedicine 11 (2016) 625.

[67] L. Li, et al., Simulation of the in vivo fate of polymeric nanoparticles traced by environment-responsive near-infrared dye: a physiologically based pharmacokinetic modelling approach, Molecules 26 (5) (2021) 1271.
[68] V. Shalgunov, et al., Comprehensive study of the drug delivery properties of poly (l-lactide)-poly(ethylene glycol) nanoparticles in rats and tumor-bearing mice, J. Control. Release 261 (2017) 31–42.
[69] D. Li, et al., Using a PBPK model to study the influence of different characteristics of nanoparticles on their biodistribution, in: Journal of Physics: Conference Series, IOP Publishing, 2013.
[70] H. Deng, et al., Multimodal nanocarrier probes reveal superior biodistribution quantification by isotopic analysis over fluorescence, ACS Nano 14 (1) (2019) 509–523.
[71] D.R. Beckford Vera, et al., PET imaging of the EPR effect in tumor xenografts using small 15 nm diameter polyethylene glycols labeled with zirconium-89 imaging of the EPR effect in tumors using 89Zr-labeled PEG, Mol. Cancer Ther. 19 (2) (2020) 673–679.
[72] G. Yang, Y. Liu, C.-X. Zhao, Quantitative comparison of different fluorescent dye-loaded nanoparticles, Colloids Surf. B: Biointerfaces 206 (2021), 111923.
[73] G. Yang, et al., Implications of quenching-to-dequenching switch in quantitative cell uptake and biodistribution of dye-labeled nanoparticles, Angew. Chem. Int. Ed. 60 (28) (2021) 15426–15435.
[74] J. Qi, et al., Towards more accurate bioimaging of drug nanocarriers: turning aggregation-caused quenching into a useful tool, Adv. Drug Deliv. Rev. 143 (2019) 206–225.
[75] Q. Shi, et al., Digital micelles of encoded polymeric amphiphiles for direct sequence reading and ex vivo label-free quantification, Nat. Chem. (2022) 1–14.
[76] N. Haddish-Berhane, J.L. Rickus, K. Haghighi, The role of multiscale computational approaches for rational design of conventional and nanoparticle oral drug delivery systems, Int. J. Nanomedicine 2 (3) (2007) 315–331.
[77] F.M. Kashkooli, et al., Nexus between in silico and in vivo models to enhance clinical translation of nanomedicine, Nano Today 36 (2021), 101057.
[78] M. Shamsi, et al., Mathematical and computational modeling of nano-engineered drug delivery systems, J. Control. Release 307 (2019) 150–165.
[79] J.L. Wu, et al., A proposed mathematical description of in vivo nanoparticle delivery, Adv. Drug Deliv. Rev. 189 (2022) 114520.
[80] P. Mascheroni, B.A. Schrefler, In silico models for nanomedicine: recent developments, Curr. Med. Chem. 25 (34) (2018) 4192–4207.
[81] Y. Gao, et al., Advances in mathematical models of the active targeting of tumor cells by functional nanoparticles, Comput. Methods Prog. Biomed. 184 (2020), 105106.
[82] C. Wilhelm, et al., Interaction of anionic superparamagnetic nanoparticles with cells: kinetic analyses of membrane adsorption and subsequent internalization, Langmuir 18 (21) (2002) 8148–8155.
[83] P. Decuzzi, M. Ferrari, Design maps for nanoparticles targeting the diseased microvasculature, Biomaterials 29 (3) (2008) 377–384.
[84] P. Decuzzi, M. Ferrari, The adhesive strength of non-spherical particles mediated by specific interactions, Biomaterials 27 (30) (2006) 5307–5314.
[85] H.-M. Ding, Y.-Q. Ma, Theoretical and computational investigations of nanoparticle–biomembrane interactions in cellular delivery, Small 11 (9–10) (2015) 1055–1071.
[86] C. De Michele, et al., Simulation and theory of antibody binding to crowded antigen-covered surfaces, PLoS Comput. Biol. 12 (3) (2016), e1004752.
[87] S. Sirin, et al., AB-bind: antibody binding mutational database for computational affinity predictions, Protein Sci. 25 (2) (2016) 393–409.
[88] D.M. Eckmann, et al., Multiscale modeling of protein membrane interactions for nanoparticle targeting in drug delivery, Curr. Opin. Struct. Biol. 64 (2020) 104–110.
[89] N. Ramakrishnan, et al., Biophysically inspired model for functionalized nanocarrier adhesion to cell surface: roles of protein expression and mechanical factors, R. Soc. Open Sci. 3 (6) (2016), 160260.
[90] J. Tan, et al., Coupled particulate and continuum model for nanoparticle targeted delivery, Comput. Struct. 122 (2013) 128–134.
[91] K. Müller, D.A. Fedosov, G. Gompper, Margination of micro- and nano-particles in blood flow and its effect on drug delivery, Sci. Rep. 4 (1) (2014) 4871.
[92] G. Fullstone, et al., Modelling the transport of nanoparticles under blood flow using an agent-based approach, Sci. Rep. 5 (1) (2015) 10649.
[93] M. Cooley, et al., Influence of particle size and shape on their margination and wall-adhesion: implications in drug delivery vehicle design across nano-to-micro scale, Nanoscale 10 (32) (2018) 15350–15364.
[94] O. Richfield, R. Cortez, L.G. Navar, Simulations of glomerular shear and hoop stresses in diabetes, hypertension, and reduced renal mass using a network model of a rat glomerulus, Phys. Rep. 8 (18) (2020), e14577.
[95] O. Richfield, R. Cortez, L.G. Navar, Simulations of increased glomerular capillary wall strain in the 5/6-nephrectomized rat, Microcirculation 28 (7) (2021), e12721.
[96] S.S. Hossain, et al., Mathematical modeling of coupled drug and drug-encapsulated nanoparticle transport in patient-specific coronary artery walls, Comput. Mech. 49 (2012) 213–242.
[97] S. Kang, et al., Modeling the binding and diffusion of receptor-targeted nanoparticles topically applied on fresh tissue specimens, Phys. Med. Biol. 64 (4) (2019) 045013.
[98] S. Sohrabi, et al., Numerical simulation of particle transport and deposition in the pulmonary vasculature, J. Biomech. Eng. 136 (12) (2014), 121010.
[99] Y. Li, et al., Multiscale modeling and uncertainty quantification in nanoparticle-mediated drug/gene delivery, Comput. Mech. 53 (3) (2014) 511–537.
[100] H.B. Frieboes, et al., A computational model for predicting nanoparticle accumulation in tumor vasculature, PLoS One 8 (2) (2013), e56876.
[101] L.T. Curtis, et al., Computational modeling of tumor response to drug release from vasculature-bound nanoparticles, PLoS One 10 (12) (2015), e0144888.
[102] I. Chamseddine, Utilizing Computational Design Optimization in Cancer Nanotherapy and Biology System Principles in Air Transportation: A Successful Demonstration of Interdisciplinary Research, McGill University (Canada), 2019.
[103] I.M. Chamseddine, H.B. Frieboes, M. Kokkolaras, Design optimization of tumor vasculature-bound nanoparticles, Sci. Rep. 8 (1) (2018) 17768.
[104] T.T. Goodman, et al., Spatio-temporal modeling of nanoparticle delivery to multicellular tumor spheroids, Biotechnol. Bioeng. 101 (2) (2008) 388–399.
[105] J. Fish, G.J. Wagner, S. Keten, Mesoscopic and multiscale modelling in materials, Nat. Mater. 20 (6) (2021) 774–786.
[106] S. Prudhomme, et al., An adaptive strategy for the control of modeling error in two-dimensional atomic-to-continuum coupling simulations, Comput. Methods Appl. Mech. Eng. 198 (21) (2009) 1887–1901.
[107] J. Liu, et al., Computational model for nanocarrier binding to endothelium validated using in vivo, in vitro, and atomic force microscopy experiments, Proc. Natl. Acad. Sci. 107 (38) (2010) 16530–16535.
[108] A. Beaussart, et al., Probing the influence of cell surface polysaccharides on nanodendrimer binding to gram-negative and gram-positive bacteria using single-nanoparticle force spectroscopy, Nanoscale 10 (26) (2018) 12743–12753.
[109] M. Leitner, et al., Atomic force microscopy imaging in turbid liquids: a promising tool in nanomedicine, Sensors 20 (13) (2020) 3715.
[110] Y. Liu, et al., Nanoparticle tension probes patterned at the nanoscale: impact of integrin clustering on force transmission, Nano Lett. 14 (10) (2014) 5539–5546.
[111] G. Pyrgiotakis, C.O. Blattmann, P. Demokritou, Real-time nanoparticle–cell interactions in physiological media by atomic force microscopy, ACS Sustain. Chem. Eng. 2 (7) (2014) 1681–1690.
[112] Y.Z. Shi, et al., Sculpting nanoparticle dynamics for single-bacteria-level screening and direct binding-efficiency measurement, Nat. Commun. 9 (1) (2018) 815.
[113] J.K. Vasir, V. Labhasetwar, Quantification of the force of nanoparticle-cell membrane interactions and its influence on intracellular trafficking of nanoparticles, Biomaterials 29 (31) (2008) 4244–4252.
[114] T. Wiegand, et al., Forces during cellular uptake of viruses and nanoparticles at the ventral side, Nat. Commun. 11 (1) (2020) 32.
[115] A.L. Van De Ven, et al., Integrated intravital microscopy and mathematical modeling to optimize nanotherapeutics delivery to tumors, AIP Adv. 2 (1) (2012), 011208.
[116] B. Davies, T. Morris, Physiological parameters in laboratory animals and humans, Pharm. Res. 10 (7) (1993) 1093–1095.
[117] C.R. Neal, et al., Novel hemodynamic structures in the human glomerulus, Am. J. Physiol. Ren. Physiol. 315 (5) (2018) F1370–F1384.
[118] T. Lysyy, et al., Ex vivo isolated human vessel perfusion system for the design and assessment of nanomedicines targeted to the endothelium, Bioeng. Transl. Med. 5 (2) (2020), e10154.
[119] S.R.R. Dos Reis, et al., Senescence and the impact on biodistribution of different nanosystems: the discrepancy on tissue deposition of graphene quantum dots, polycaprolactone nanoparticle and magnetic mesoporous silica nanoparticles in young and elder animals, Pharm. Res. 37 (3) (2020) 40.
[120] J. Lazarovits, et al., Synthesis of patient-specific nanomaterials, Nano Lett. 19 (1) (2018) 116–123.
[121] Y. Jiang, et al., A "top-down" approach to actuate poly(amine-co-ester) terpolymers for potent and safe mRNA delivery, Biomaterials 176 (2018) 122–130.
[122] M. Tavares Luiz, et al., Design of experiments (DoE) to develop and to optimize nanoparticles as drug delivery systems, Eur. J. Pharm. Biopharm. 165 (2021) 127–148.
[123] Y.H. Bae, K. Park, Targeted drug delivery to tumors: myths, reality and possibility, J. Control. Release 153 (3) (2011) 198–205.
[124] P. Dogra, et al., Establishing the effects of mesoporous silica nanoparticle properties on in vivo disposition using imaging-based pharmacokinetics, Nat. Commun. 9 (1) (2018).
[125] P. Dogra, et al., Image-guided mathematical modeling for pharmacological evaluation of nanomaterials and monoclonal antibodies, Wiley Interdiscip. Rev. Nanomed. Nanobiotechnol. 12 (5) (2020), e1628.
[126] G.T. Tietjen, et al., Focus on fundamentals: achieving effective nanoparticle targeting, Trends Mol. Med. 24 (7) (2018) 598–606.
[127] K. Park, Facing the truth about nanotechnology in drug delivery, ACS Nano 7 (9) (2013) 7442–7447.